Int. J. Heat Mass Transfer. Vol. 18, pp. 433–441. Pergamon Press 1975. Printed in Great Britain

TRANSPIRATION COOLING OF A ROTATING DISK: AN EXPERIMENTAL STUDY

WILLIAM P. COSART*
Department of Chemical Engineering, University of Arizona, Tucson, Arizona, U.S.A.

(*Received* 14 *September* 1973 *and in revised form* 18 *April* 1974)

Abstract—Heat-transfer coefficients were experimentally determined for a transpiration-cooled rotating disk. A theoretical analysis by previous investigators, based on an assumption of constant properties, was inadequate for predicting results in the present study of air injected into an air environment. However, a simple density ratio was sufficient to realign predicted and experimental results. The range of experiments included injection rates of 0·35–1·04 lb/min ft^2 and rotation Reynolds numbers of 19 000–51 000. The ratio of h/h_0 (h_0 = coefficient for impermeable disk) varied from 0·69 to 0·21. Over the range studied, a semi-logarithmic equation correlates the data within 10 per cent.

NOMENCLATURE

A, area of disk [ft^2];
C_f, skin friction coefficient [dimensionless];
C_p, heat capacity [Btu/lb degF];
F, non-dimensional radial velocity [dimensionless];
G, non-dimensional circumferential velocity [dimensionless];
Gr, Grashof number [dimensionless];
h, heat-transfer coefficient [Btu/h ft^2 degF];
H, non-dimensional axial velocity [dimensionless];
H, distance from disk to stationary surface opposite [ft];
k, thermal conductivity [Btu/h ft degF];
n, mass flux [lb/h ft^2];
Nu, Nusselt number [dimensionless];
Pr, Prandtl number [dimensionless];
q, energy flux [Btu/h ft^2];
r, radial distance [ft];
R, radius of disk [ft];
Re, Reynolds number [dimensionless];
Sc, Schmidt number [dimensionless];
t, time [hr];
T, temperature [°R];
U, velocity [ft/h];
v, velocity [ft/h].

Greek symbols

δ, boundary-layer thickness [ft];
ε, emissivity [dimensionless];
η, non-dimensional axial distance [dimensionless];
θ, non-dimensional temperature [dimensionless];
θ_T, ratio h/h_0 [dimensionless];
μ, viscosity [lb/ft h];
ν, kinematic viscosity [ft^2/h];
ρ, density [lb/ft^3];
σ, Stefan–Boltzmann constant [Btu/h ft^2 °R^4];
ϕ, non-dimensional weight fraction [dimensionless];
ω, rotational rate [h^{-1}].

Subscripts

c, injectant at the inlet to the plenum below the porous surface;
cw, average of c and w conditions;
in, same as subscript c;
0, zero injection;
w, condition at porous surface;
$w\infty$, condition at surface of surrounding;
∞, condition far from porous surface.

INTRODUCTION

TRANSPIRATION cooling is a means of cooling by injection of a fluid through a porous surface. During the last 20 years, transpiration cooling has been the subject of scores of scientific and engineering studies. High interest has been shown in the topic from both the practical and theoretical standpoint.

Transpiration cooling is of theoretical interest in fluid mechanics because fluid injected into a boundary layer obviously alters the flow conditions near the wall. Since temperature and concentration profiles are dependent on the velocity field, the entire character of the boundary layer is affected.

A thorough review of the hundreds of individual theoretical contributions to the widely studied field of

*Formerly at Oregon State University, where this work was initiated.

transpiration cooling is beyond the scope of this paper. Fortunately, several excellent reviews already exist, for example Gross *et al.* [1] in 1961 (see also Sparrow *et al.* [2]), Gross [3] 1967, and three very broad papers in 1972 by Mills and Wortman [4], Wortman, Mills and Hoo [5], and Kays [6].

The practical importance of transpiration cooling arises due to the dramatic decrease of heat-transfer coefficient caused by injection. The possibility of protecting solid materials exposed to very hot fluids has long attracted engineers who wish to improve thermodynamic efficiency by increasing the temperature of the working fluid still further. This has stimulated the study of such practical applications as combustion chamber walls, gas turbine blades and disks, rocket nozzles, hypersonic ram-jet intakes, etc.

The particular geometry chosen for the study of transpiration cooling reported herein is the rotating disk. The rotating disk itself has been the subject of many investigations, again for practical as well as theoretical reasons. From the practical standpoint, the rotating disk represents a mechanically simple model for such complex items of equipment as turbine disks, fan blades, or centrifugal pumps. From the theoretical standpoint, the disk is of interest since the boundary layer induced by its rotation exhibits three dimensional flow which can be treated by the full Navier–Stokes equations (i.e. no terms are left out as in the two-dimensional boundary-layer equations).

The literature on the rotating disk is quite extensive and will not be reviewed in detail here. The reader is referred to papers by von Karman [7], Cochran [8], Ostrach and Thornton [9], Schwiderski and Lugt [10], Benton [11], and Homsy and Hudson [12] for theoretical analyses and calculations concerning the fluid mechanics of the problem. Early flow measurements are summarized in Goldstein [13], Schlichting [14], and Dorfman [15], including the work of Theodorson and Regier [16], Gregory and Walker [17], and Smith [18]. Cham and Head [19] report the results of more recent experiments.

The rotating disk geometry has been the subject of many energy and mass-transfer investigations. Because the disk is a model of the gas turbine disk, heat transfer has been studied extensively, and because it provides a simple and effective tool for measuring reaction rates, diffusivities, and electrochemical transference numbers in liquid systems (see Levich [20] for example), mass transfer has also received much attention.

An early theoretical study of heat transfer was that of Wagner [21] in 1948. For laminar flow, assuming constant properties, Wagner solved integral equations for the temperature distribution, finding that temperature depended on z, but was independent of r. He concluded that Nusselt number, defined as $h\delta/k$, where $\delta = (\nu/\omega)^{1/2}$, was equal to 0·34 and independent of the Reynolds number. Other theoretical investigations include those of Ostrach and Thornton [9], Lugt and Schwiderski [22], and Andrews and Riley [23]. The rotating disk was included as a special case of the rotating cone in papers by Tien and Tsuji [24], Fox [25], and Hering and Grosh [26].

Experimental heat- and mass-transfer measurements were reported by Young [27], Cobb and Saunders [28], Kreith, Taylor and Chong [29], and Richardson and Saunders [30].

The effect of both suction and injection on the flow, heat transfer, and mass transfer from a rotating disk was studied by Sparrow and Gregg [31]. This paper used the transformation of variables common to most rotating disk work, normalizing axial distance with boundary-layer thickness $\eta = z/\delta$, where $\delta = (\nu/\omega)^{1/2}$, and non-dimensionalizing the dependent variables in the following way:

$$F(\eta) = \frac{v_r}{r\omega} \qquad P(\eta) = \frac{p}{\mu\omega}$$

$$G(\eta) = \frac{v_\theta}{r\omega} \qquad \theta(\eta) = \frac{T - T_\infty}{T_w - T_\infty}$$

$$H(\eta) = \frac{v_z}{(\omega\nu)^{1/2}} \qquad \phi(\eta) = \frac{W_1 - W_{\infty}}{W_{1_w} - W_{1_\infty}}.$$

Assuming constant properties, velocity, temperature and mass fraction profiles were calculated, from which Nusselt numbers were determined. Thus, reference [31] gives the theoretical results against which the experimental data in the present paper are compared.

EXPERIMENTAL

Rotating disk

An apparatus to measure heat-transfer coefficients was built. Heated air was pumped to a rotating plenum chamber, which was designed to distribute the air evenly through a porous surface into an air environment. Figure 2 is a schematic of the overall system,

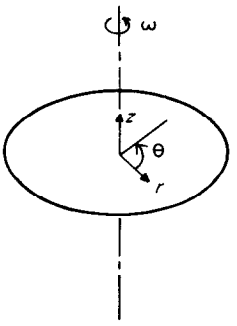

FIG. 1. Rotating disk coordinates.

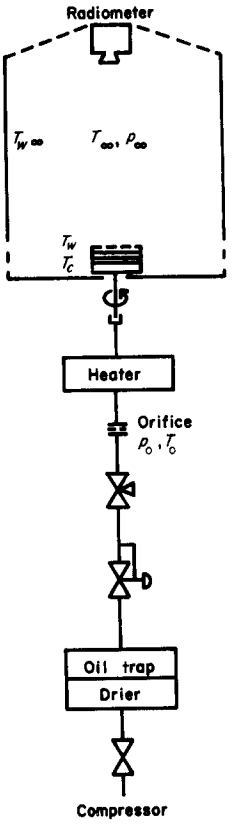

FIG. 2. Schematic flow diagram, indicating variables measured.

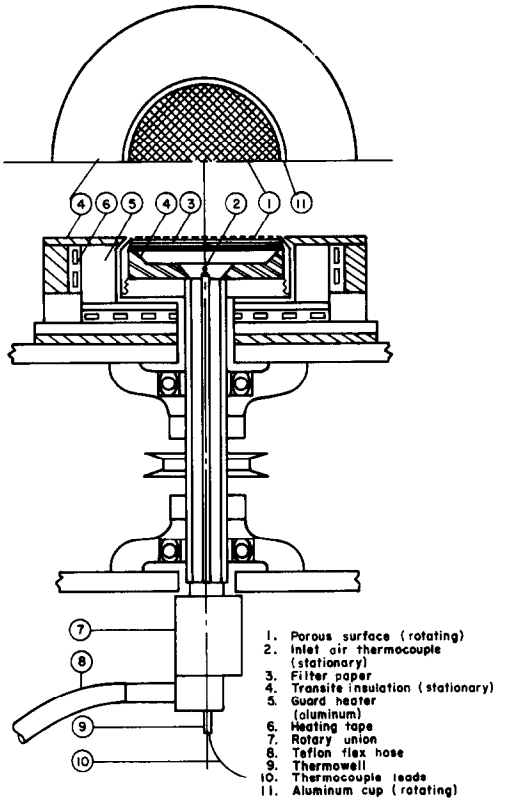

FIG. 3. Details of rotating apparatus.

and Fig. 3 gives details of the rotating disk and plenum chamber. Items of special interest will be discussed below. More details can be found in [32].

Air flow was measured by an orifice meter, calibrated to 0·5 per cent. Temperature of the air entering the rotary coupling was controlled by a proportional controller. The rotary coupling itself was a commercially available item and was found to leak less than 0·5 per cent of the injection flow rate. An electronically controlled half horsepower DC motor drove the rotating apparatus through a fan belt–pulley arrangement. Rotational rate was measured with a strobe-tachometer.

Figure 2 shows that the plenum chamber below the disk was insulated and had a guard heater to minimize radial energy loss. Immediately below the disk are twelve thicknesses of high grade fiberglass filter paper, sufficient to provide a pressure drop of 116 torr at the highest flow rates, thus insuring a uniform velocity distribution across the disk. The disk itself was 0·005-in thick 200 × 1400 mesh stainless steel. This "mesh" was opaque to visible light. It was crimped and glued with epoxy cement to fit smoothly and tightly across the top of the aluminum cup which held the entire assembly together. The top edge of the cup was beveled to allow the boundary layer to leave the disk smoothly. For the same purpose, the top of the guard heater was insulated with smooth transite, and was placed slightly below the plane of the disk.

Enclosure

In order to protect the boundary layer induced by the rotation of the disk from external convection currents, an enclosure $22 \times 22 \times 40$ in was placed around the apparatus. The interior of the enclosure was painted black except for the top and part of the lower edge, which were covered with porous material. This material allowed the enclosure to "breathe", but still prevented light and convection currents from the laboratory from entering the box.

A careful reading of the literature will indicate that the enclosure is large enough not to affect the flow induced by the rotating disk. It is apparent that three boundary layers may be established: (1) on the disk itself, (2) on the enclosure surface normal to the disk, and (3) on the enclosure surface parallel to the disk. These boundary layers will not interact if sufficiently separated.

Upon leaving the outermost radius of the rotating

disk, boundary layer (1) develops into a radial jet within about 0·1–0·4 radii [33, 30]. Both theory [33] and measurement [30] indicate a rapid decay to negligible velocities within 2–4 radii. Since the square enclosure used in this study had sides 5·6 times the disk diameter, it is apparent that no interference is expected between boundary layers (1) and (2).

Flow patterns in an enclosure depend significantly on axial clearance between the disk and the stationary surface opposite the disk. When the two surfaces are very close, boundary layers (1) and (3) merge into couette flow. For somewhat greater separation, the flow is visualized as two individual boundary layers separated by a central core of fluid rotating as a body at constant angular velocity [10, 34]. The value of the angular velocity of this core is some fraction of that of the rotating disk, and depends on the clearance. Some investigators indicate the important parameter is the ratio of clearance to diameter, while others contend that it is "clearance Reynolds number", $\omega H^2/\nu$.

Extrapolation of the data of Daily and Nece [34] indicates decay to zero core velocity at a separation somewhat less than one disk diameter. Calculations by Tomlan and Hudson [35] indicate substantial though rapidly decaying interaction at one diameter. However, mass-transfer results by Kreith, Taylor, and Chong [29] with a naphthalene disk in air indicated only a 10 per cent lowering of Sherwood number with separation of 0·25 diameter. Since the clearance for the present apparatus is ten times the diameter, negligible interference would be expected.

The argument that clearance Reynolds number is the important parameter was proposed by Lehmkuhl and Hudson [36] in their study measuring the dissolution of cinnamic acid in water. They found no effect on Sherwood number for $\omega H^2/\nu > 50$. Flow visualization studies by the same authors indicated interaction of hydrodynamic boundary layers below a clearance Reynolds number of 430. Care must be used in extrapolating this conclusion quantitatively to other systems, however, for the Schmidt number of the system studied was approximately 600, indicating a mass transfer boundary layer much thinner than the momentum boundary layer. If, for order-of-magnitude estimation, Schmidt number dependence is assumed proportional to $Sc^{-1/3}$, then no interference with heat or mass transfer would be expected above a clearance Reynolds number of 4000–5000 for $Sc = Pr = 0{\cdot}7$. Clearance Reynolds numbers in the present experiments were always greater than 7×10^6. Again, the conclusion is that negligible interference is expected.

Temperature measurement

All temperatures measured, except those of the rotating disk surface, were determined by calibrated iron–constantan thermocouples, using an integrating digital voltmeter. The voltmeter was checked to 1 μV each day against a specially aged and stable zener diode, which was an integral component within the instrument. The voltmeter was considered accurate to at least 3 μV (0·1°F). A carefully built ice bath was used as a reference temperature for the thermocouple measurements.

The temperature of the porous surface was measured with an infrared radiometer manufactured by Irtronics, Inc., Stamford, Connecticut. The instrument had a telescopic sight for aligning the detector on the spot where the temperature was to be measured. At 40 in its field of view was a circle 0·75 in dia. The lead sulfide infrared detector was sensitive to wavelengths from 1·9 to 2·9 microns. The instrument was connected to a constant voltage transformer to avoid direct connection to line voltage and to stabilize its power source.

To obtain the sensitivity and range required, it was necessary to modify the bias on the lead sulfide detector from the value set by the manufacturer. The emissivity correction was set at the lowest possible value, then the bias was set at 75 V. This permitted measurement of temperatures in the range 125–200°F. Sensitivity varied from about 0·1 mV/°F at 130°F to about 0·6 mV/°F at 180°F. The instrumentation output, 0–5 mV, was transmitted by shielded cable to a second integrating digital voltmeter. Very slow drift of the radiometer indicated that daily calibration was sufficient to provide the required accuracy and reproducibility.

Infrared calibration

Calibration of the radiometer was effected by aiming it at a two-inch diameter stationary disk made of stainless steel mesh from the same lot as the rotating disk. This stationary calibration disk was mounted in a corner of the enclosure during calibration only, then removed before a rotational run was started. It had a guard heater wrapped with a heating tape regulated by a variable transformer. Spot welded to the underside of the disk were three thermocouples. Power to the guard heater was adjusted to make the disk isothermal, as indicated by the three thermocouples.

Output of the radiometer was affected by instrument temperature and by mechanical vibration. These effects were essentially eliminated as follows:

The instrument was warmed up at least 24 h before calibration and data-taking, and 70°F water was circulated through an internal cooling chamber. In this way, the instrument's operating temperature was maintained constant. A "standard vibration" was provided by turning the disk a minimum of 1500–2000 rev/min.

In this way calibration and heat-transfer data were affected identically.

Upon completion of a calibration of the radiometer, the heated air was passed through the rotating disk until steady state was attained. This condition was presumed when temperatures remained essentially unchanged for 15–20 min. No data were accepted unless the radiometer indicated the center of the disk and the edge were the same temperature (within 0·3–0·5 degF, as close as reproducibility of the radiometer warranted). Isothermality was achieved by adjusting the guard heater. Several hours were required to reach an isothermal steady state.

RESULTS

Experimental results are presented in Table 1 and Figs. 5–9. Temperature and flow data are converted to heat-transfer coefficients using an energy balance around the disk and plenum chamber.

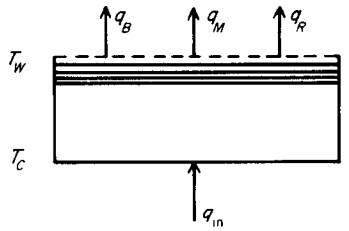

FIG. 4. Energy balance on rotating disk and plenum chamber.

Assuming negligible energy loss radially because of the guard heater and the insulation, only axial terms are required, as shown in Fig. 4. Energy into the control volume is merely that transported by air entering the plenum, q_{in}. This term is equated to the energy out of the control volume, namely q_B, the air leaving the porous surface, q_m, the molecular contribution

$$\left(-k\frac{dT}{dz}\bigg|_{z=0} = h\{T_w - T_\infty\}\right),$$

and q_R, radiation. The resulting equation is

$$h = \frac{n_w \hat{C}_{P_{cw}}(T_c - T_w) - \sigma\varepsilon(T_w^4 - T_{w\infty}^4)}{T_w - T_\infty}. \quad (1)$$

Calculating h this way tacitly assumes that all of the disk which loses heat by convection is porous. However, this was not the case in the apparatus. A thin ring around the outer edge of the disk was exposed to the surrounding environment, but was not permeable (see Fig. 3). Because of this non-porous area (equivalent to 11·9 per cent of the porous area), a correction must be applied to the heat-transfer coefficient calculated by equation (1).

Two methods of correcting for the impermeable portion of the disk were considered:

(a) Since the outer ring is not porous, it could be argued that the heat transfer coefficient for that area is h_0, i.e. the coefficient obtained for zero injection.

Table 1. Experimental results

Rev/min	n (lb/min ft^2)	Re	h* (Btu/h ft^2 °F)	h† (Btu/h ft^2 °F)	Nu	H_w	$\frac{\rho_w}{\rho_\infty} H_w$	θ_T h/h_0	$\frac{Gr}{Re^2}$
1520	0·440	20 300	2·59	2·04	0·144	0·668	0·611	0·51	6·82(10^{-4})
1500	0·480	19 500	2·33	1·78	0·127	0·900	0·801	0·45	9·27
1500	0·723	18 600	1·89	1·333	0·095	1·142	0·989	0·344	11·45
1520	1·045	19 000	1·43	0·868	0·062	1·631	1·428	0·224	10·27
2150	0·362	29 900	4·02	3·38	0·201	0·456	0·427	0·69	4·25(10^{-4})
2050	0·438	27 600	3·55	2·92	0·178	0·571	0·526	0·62	3·54
2040	0·579	26 500	3·13	2·50	0·153	0·769	0·690	0·54	4·55
2040	0·734	25 900	2·96	2·32	0·142	0·981	0·869	0·51	5·17
2040	0·733	26 000	2·88	2·24	0·137	0·982	0·866	0·49	5·39
2050	1·044	25 600	1·70	1·063	0·065	1·406	1·224	0·246	5·91
2050	1·044	25 600	1·58	0·947	0·058	1·406	1·225	0·210	5·84
3010	0·348	41 400	4·26	3·51	0·177	0·373	0·346	0·61	1·81(10^{-4})
3020	0·727	38 400	3·54	2·78	0·140	0·801	0·708	0·50	2·41
3030	0·728	38 400	3·40	2·64	0·133	0·801	0·707	0·48	2·43
3010	1·043	37 500	2·34	1·58	0·080	1·161	1·009	0·29	2·77
4000	0·348	54 600	5·11	4·25	0·186	0·324	0·300	0·65	0·89(10^{-4})
4000	0·348	54 600	5·21	4·35	0·190	0·324	0·300	0·66	0·88
4000	0·727	50 200	4·42	3·55	0·155	0·698	0·613	0·56	1·45
4000	1·043	49 700	3·11	2·24	0·098	1·008	0·874	0·354	1·66
4000	1·041	49 600	3·46	2·59	0·113	1·008	0·873	0·41	1·60

*Uncorrected using equation (1).

†Corrected, assuming coefficient for non-porous area equals h_0.

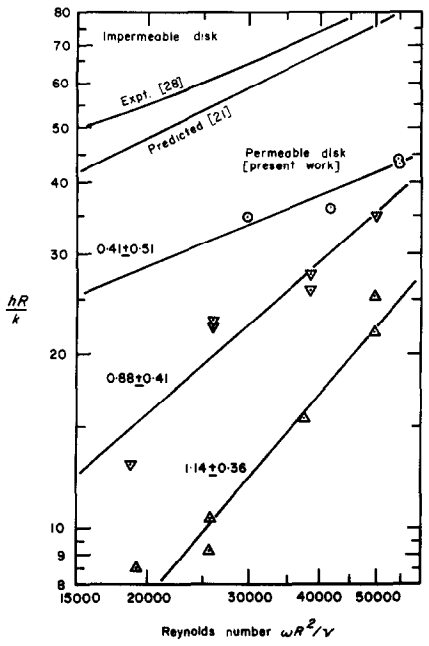

FIG. 5. Effect of Reynolds number and injection on heat transfer. Least-squares slope ±90 per cent confidence interval shown. ○, 0·35 lb/min ft²; ▽, 0·73 lb/min ft²; △, 1·04 lb/min ft².

(b) Since the air injected through the porous disk immediately obtains a radial velocity component (boundary-layer thickness $\delta = (\nu/\omega)^{1/2}$ is a few hundredths of an inch), causing the injection to flow over the non-porous area, it could be argued that the non-porous area is film-cooled; furthermore that the film-cooling coefficient is approximately the same as the transpiration cooling coefficient. This argument would lead to the conclusion that the heat-transfer coefficient is essentially the same over both the porous and the non-porous areas of the disk.

The two assumptions described above represent two extremes. The author feels that assumption (b) would represent the physical situation across the top of the disk if the guard heater were not present, but that edge effects (such as those described by Richardson and Saunders [30]) probably induce a heat-transfer coefficient for the non-porous area higher than one would expect for pure transpiration cooling. Thus it is felt that assumption (a) probably gives a more accurate correction than assumption (b) and, therefore, correction (a) is applied to the data in all of the correlations and figures that follow.

DISCUSSION

Figure 5 presents the data as hR/k vs Reynolds number for each of three injection rates. Previous results for impermeable disks are included for comparison. The lowering of h due to transpiration is apparent in this figure.

Previous work by Wagner [21] and Sparrow and Gregg [31] has used the grouping $h\delta/k$ rather than hR/k. These two dimensionless groups are related by the expression $h\delta/k = (hR/k)Re^{-1/2}$. Thus, $h\delta/k$ for a rotating disk is analogous to the grouping $NuRe^{-1/2}$ used to correlate flat plate heat-transfer results (see [37] for example).

Wagner concluded that Nu (defined as $h\delta/k$) should be independent of Re for an impermeable disk, showing that Nu should be a function of injection rate only, but not of Re. If Nu were independent of Re, then hR/k should be proportional to $Re^{1/2}$ for a given injection rate, i.e. the data should fall on lines of slope 0·5 in Fig. 5. While the data for any single injection

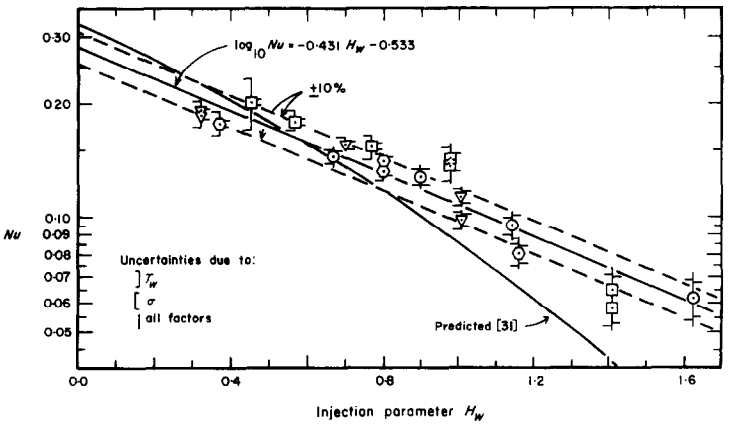

FIG. 6. Nusselt number dependence on injection parameter H_w. ○, 1500 rev/min; □, 2000 rev/min; ⊙, 3000 rev/min; ▽, 4000 rev/min.

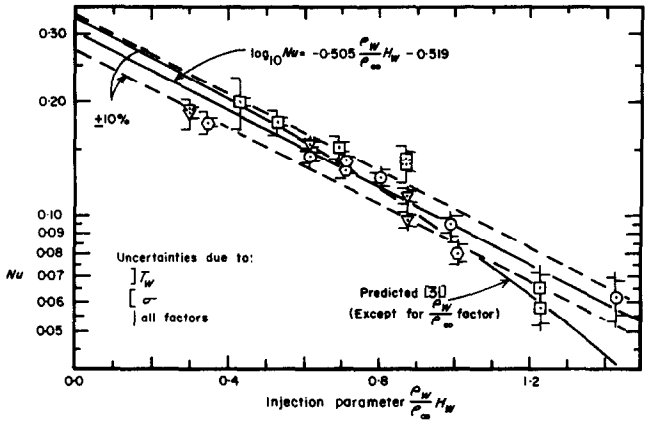

FIG. 7. Nusselt number dependence on injection parameter $(\rho_w/\rho_\infty)H_w$. (See Fig. 6 for rotation rates.)

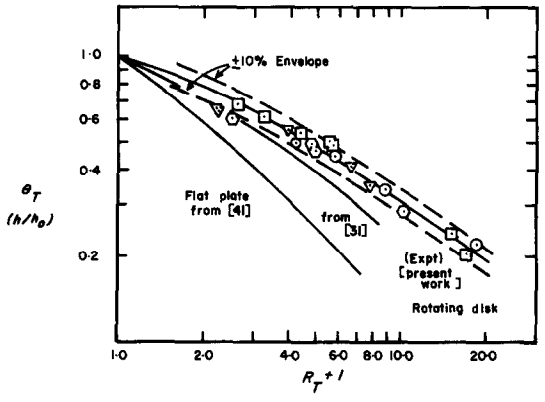

FIG. 8. The ratio h/h_0 vs R_T. ○, $Re = 19\,000$; □, $Re = 26\,000$; ◇, $Re = 39\,000$; ▽, $Re = 51\,000$.

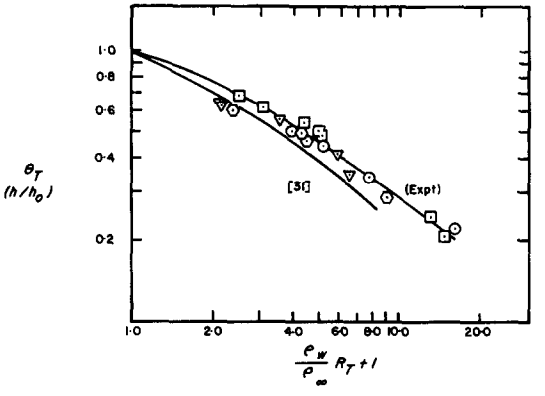

FIG. 9. The ratio h/h_0 vs $(\rho_w/\rho_\infty)R_T$. (See Fig. 8 for rotational Reynolds number.)

rate have appreciable scatter (accentuated by the scale of the figure), nonetheless every point lies within 20 per cent of the least-squares line shown. The spread of the data precludes a definitive or quantitative conclusion, but qualitatively the slope appears to be about one-half at low injection rates and appears to increase at higher injection rates. A similar tentative conclusion is drawn by Elzy [38] for stagnation point heat-transfer coefficients for a cylinder in cross-flow with transpiration.

As mentioned above, $h\delta/k$ for the rotating disk is analogous to $NuRe^{-1/2}$ for flat plate boundary layers. The grouping $h\delta/k$ is referred to as Nu by Sparrow and Gregg [31] and others, and will be called Nu in further discussion here. Previous transpiration calculations (e.g. Gross *et al.* [1]) have plotted results using a blowing parameter, $(\rho_w V_w/\rho_\infty U_\infty)Re^{1/2}$. Replacing U_∞ by ωR, a similar blowing parameter becomes $(\rho_w/\rho_\infty)V_w/(\omega\nu)^{1/2}$ or $(\rho_w/\rho_\infty)H_w$ in terms of rotating disk variables. Figure 7 shows the present data plotted as Nu vs $(\rho_w/\rho_\infty)H_w$. For comparative purposes, the data are also plotted as Nu vs H_w in Fig. 6. H_w is the blowing parameter proposed by Sparrow and Gregg [31] in their constant property analysis.

Figures 6 and 7 show the advantage of presenting all the experimental data together, rather than showing individual injection rates separately as in Fig. 5. It should be noted that rotational rate ω is submerged in both the ordinate and abscissa of Figs. 6 and 7. Semi-logarithmic coordinates were chosen so that extrapolation to zero injection along the abscissa would be possible, and so that brackets of equal percent error would be represented by equal vertical distances anywhere on the graph.

For the range of experimentation, the data are reasonably well-correlated by an equation of the form

$$\log Nu = BX + C$$

where X represents the blowing parameter. Nearly all of the data fall within a ± 10 per cent envelope, indicating the adequacy of this method of correlation. The particular values of B and C for the equation are found on each figure and depend on the choice of blowing parameter.

Figure 7 brings the experimental data closest to the curve predicted by Sparrow and Gregg [31]. It is interesting to note that Fig. 6, which uses the blowing parameter proposed by constant property analysis, shows a rather poor correspondence between predicted curve and experiment; whereas Fig. 7, which uses a blowing parameter with a "correction" for *variable* properties, shows a reasonably good correspondence to the *constant* property prediction.

Estimated uncertainties in the data are shown in Figs. 6 and 7 by horizontal brackets and vertical lines. The brackets facing left indicate the result of recalculating Nu with a reasonable estimate of the experimental error in measuring T_w. The brackets facing right result from recalculating Nu assuming emissivity was $0{\cdot}30 \pm 0{\cdot}05$. The author could not measure emissivity using the method described in references [38] and [39]. Therefore the value of 0·3 was assumed because Elzy [38] measured that value for the same type of material made by the same manufacturer. Sensitivity to the value of ε is shown by the brackets facing right. The total uncertainty in the data is indicated by the vertical line. The upper and lower bounds in total uncertainty were calculated by summing the squares of the individual uncertainties (see Davies [40], for example).

A measure of effectiveness for transpiration cooling is h/h_0, where h_0 represents the heat-transfer coefficient with no injection. Bird, Stewart and Lightfoot [41], p. 676, call this ratio θ_T, and plot θ_T as a function $R_T = n_w C_p/h$. Their plot is for laminar flow over a flat plate.

To permit a comparison of effectiveness of transpiration cooling for a rotating disk to effectiveness for a flat plate, the curve from Bird *et al.* is reproduced if Figs. 8 and 9, the rotating disk results predicted by Sparrow and Gregg are presented, and data obtained in this work are given on the same graphs. Figure 8 uses R_T in the abscissa, while Fig. 9 uses $(\rho_w/\rho_\infty)R_T$.

To plot the experimental data in Figs. 8 and 9, h_0 had to be determined for each Reynolds number. Since h for zero injection could not be measured directly with the apparatus, the extrapolation value of $Nu_0 = 0{\cdot}302 \pm 0{\cdot}017$ (98 per cent confidence limits) from Fig. 7 was used.

Two final points of discussion of the data concern natural convection and transition from laminar to turbulent flow.

As pointed out by Richardson and Saunders [30], the ratio Gr/Re^2 arises when the equation of motion including buoyancy terms is made non-dimensional. This grouping is a measure of the interference of natural convection with forced convection heat transfer. According to the experimental results of Richardson and Saunders [30] and the calculations of Fox [25], essentially no effect is to be expected for Gr/Re^2 as low as 0·01. Since the highest value for any run in the present experiments was 0·00115, no corrections were made for natural convection.

Likewise, no allowance was made for the tendency of injection to destabilize what would otherwise be laminar flow. While the highest Re encountered in this work (55 000) is less than one-third the Re at the beginning of transition (185 000–285 000) reported by Cham and Head [19], it cannot be said *a priori* that flow was laminar throughout the present measurements. No velocity or turbulence measurements were made. It may be that the divergence between the theory [31], assuming laminar flow, and the experimental data is due to the existence of turbulence on the disk. Qualitatively, the beginnings of turbulence would tend to raise h more at higher Re and at higher injection rates. This may explain why the divergence is greater at higher values of the blowing parameter in Figs. 6 and 7. It may also explain the increase of slope (increased Re dependence) with increased injection shown in Fig. 5. One would expect to see a more obvious discontinuity on the curve for a particular injection rate if a wider range of Re were encountered and if the lowest Re values were assuredly laminar. Since the present data do not resolve these equations, it is apparent that the effect of injection on transition is an important area for further measurements.

SUMMARY AND CONCLUSIONS

As a result of the experimental work described herein, the following conclusions can be drawn:

1. For an injection parameter, the grouping $(\rho_w/\rho_\infty)H_w$ is more consistent with previous methods of correlating transpiration variables than H_w.

2. Sparrow and Gregg's results may be used to calculate the heat transfer coefficients for a rotating disk *provided* the blowing parameter $(\rho_w/\rho_\infty)H_w$ is substituted for H_w.

3. The experimental data for transpiration cooling of a rotating disk for injecting air into an air environment may also be correlated with the equation

$$\log_{10} Nu = -0{\cdot}0505 \frac{\rho_w}{\rho_\infty} H_w - 0{\cdot}519$$

over the range

$$0{\cdot}3 < \frac{\rho_w}{\rho_\infty} H_w < 1{\cdot}3.$$

4. Transpiration at a given injection rate affects heat transfer from a rotating disk less than it affects heat transfer from a flat plate.

REFERENCES

1. J. F. Gross, J. P. Hartnett, D. J. Masson and C. Gazley, Jr., A review of binary boundary-layer characteristics, *Int. J. Heat Mass Transfer* **3**, 198–221 (1961).
2. E. M. Sparrow, C. J. Scott, R. J. Forstrom and W. A. Ebert, Experiments on the diffusion-thermo effect in a binary boundary layer with injection of various gases, *J. Heat Transfer* **87**, 321–328 (1965).
3. C. Forbes Dewey, Jr. and J. F. Gross, Exact similar solutions of laminar boundary-layer equations, *Adv. Heat Transfer* **4**, 317–446 (1967).
4. A. F. Mills and A. Wortman, Two-dimensional stagnation point flows of binary mixtures, *Int. J. Heat Mass Transfer* **15**, 969–987 (1972).
5. A. Wortman, A. F. Mills and G. Soo Hoo, The effect of mass transfer on recovery factors in laminar boundary-layer flows, *Int. J. Heat Mass Transfer* **15**, 443–456 (1972).
6. W. M. Kays, Heat transfer to the transpired turbulent boundary layer, *Int. J. Heat Mass Transfer* **15**, 1023–1044 (1972).
7. T. von Karman, Uber laminare und turbulente Reibung, *Z. Angew. Math. Mech.* **1**, 233–252 (1921). (Translated in U.S. National Advisory Committee for Aeronautics Technical Memorandum No. 1092 (1946) 39p.)
8. W. G. Cochran, The flow due to a rotating disk, *Proc. Camb. Phil. Soc.* **30**, 365–375 (1934).
9. S. Ostrach and P. P. Thornton, Compressible laminar flow and heat transfer about a rotating isothermal disk. Washington, D.C., U.S. National Advisory Committee for Aeronautics, Tech. Note No. 4320 18 pp. (1958).
10. F. Schultz-Grunow, Die Reibungwiderstand rotierender Scheiben in Gehausen, *Z. Angew. Math. Mech.* **15**, 191–204 (1935).
11. Edward R. Benton, On the flow due to a rotating disk, *J. Fluid Mech.* **24**, 781–800 (1966).
12. G. M. Homsy and J. L. Hudson, Transient flow near a rotating disk, *Appl. Scient. Rev.* **18**, 384–397 (1968).
13. S. Goldstein (editor), *Modern Developments in Fluid Mechanics*, 2 Vols. Oxford University Press, London (1938).
14. H. Schlichting, *Boundary Layer Theory*, 4th edn. McGraw-Hill, New York (1960).
15. L. A. Dorfman, *Hydrodynamic Resistance and the Heat Loss of Rotating Solids*. Oliver and Boyd, Edinburgh (1963).
16. T. Theodorsen and A. Regier, Experiments on drag of revolving disks, cylinders, and streamline rods at high speeds, Washington, D.C., U.S. National Advisory Committee for Aeronautics, Technical Report No. 793, from Thirteenth Annual Report, pp. 367–384 (1944).
17. N. Gregory, J. T. Stuart and W. S. Walker, On the stability of three-dimensional boundary layers with application to flow due to a rotating disk, *Phil. Trans. R. Soc.* **A248**, 155–199 (1956).
18. N. H. Smith, Exploratory investigations of laminar boundary layer oscillations on a rotating disk, Washington, D.C., U.S. National Advisory Committee for Aeronautics, Technical Note No. 1227 (1947).
19. T. S. Cham and M. R. Head, Turbulent boundary-layer flow on a rotating disk, *J. Bas. Engng* **93**, 199–204 (1969).
20. V. G. Levich, *Physicochemical Hydrodynamics*. Prentice-Hall, Englewood Cliffs (1962).
21. C. Wagner, Heat transfer from a rotating disk to ambient air, *J. Appl. Phys.* **19**, 837–839 (1948).
22. H. J. Lugt and E. W. Schwiderski, Temperature distributions in rotating flows normal to a flat surface, *Q. Appl. Math.* **23**, 133–150 (1965).
23. R. D. Andrews and N. Riley, Unsteady heat transfer from a rotating disk, *Q. Jl Mech. Appl. Math.* **22**, 19–38 (1969).
24. C. L. Tien and J. Tsuji, Heat transfer by laminar forced flow against a non-isothermal rotating disk, *Int. J. Heat Mass Transfer* **7**, 247–252 (1964).
25. J. Fox, Effects of buoyancy on the laminar flow from an isothermal cone rotating in a quiet fluid, *J. Heat Transfer* **86**, 560 (1964).
26. R. G. Hering and R. J. Grosh, Laminar combined convection from a rotating cone, *J. Heat Transfer* **85**, 29–34 (1963).
27. R. L. Young, Heat transfer from a rotating plate, *Trans. Am. Soc. Mech. Engrs* **78**, 1163–1168 (1956).
28. E. C. Cobb and O. A. Saunders, Heat transfer from a rotating disk, *Proc. R. Soc.* **A236**, 343–351 (1956).
29. F. Kreith, J. H. Taylor and J. P. Chong, Heat and mass transfer from a rotating disk, *J. Heat Transfer* **81**, 153–163 (1963).
30. P. D. Richardson and O. A. Saunders, Studies of flow and heat transfer associated with a rotating disk, *J. Mech. Engng Sci.* **5**, 336–342 (1963).
31. E. M. Sparrow and J. L. Gregg, Mass transfer, flow and heat transfer about a rotating disk, *J. Heat Transfer* **82**, 294–302 (1960).
32. W. P. Cosart, Transpiration cooling of a rotating disk, Ph.D. Dissertation, Oregon State University (1972).
33. R. C. Chanaud, Measurements of mean flow velocity beyond a rotating disk, *J. Bas. Engng* **93**, 199–204 (1969).
34. J. W. Daily and R. E. Nece, Chamber dimension effects on induced flow and frictional resistance of enclosed rotating disks, *J. Bas. Engng* **82**, 217–232 (1960).
35. P. F. Tomlan and J. L. Hudson, Flow near an enclosed rotating disk: analysis, *Chem. Engng Sci.* **26**, 1591–1600 (1971).
36. G. D. Lehmkuhl and J. L. Hudson, Flow and mass transfer near an enclosed rotating disk: Experiment, *Chem. Engng Sci.* **26**, 1601–1613 (1971).
37. J. G. Knudsen and D. L. Katz, Fluid dynamics and heat transfer. McGraw-Hill, New York (1958).
38. E. Elzy, Transpiration cooling of a cylinder in crossflow, Ph.D. Dissertation, Oregon State University (June 1967).
39. O. E. Tewfik and J.-W. Yang, Emissivity measurements of porous materials, *J. Heat Transfer* **C85**, 79–80 (1963).
40. O. L. Davies (editor), *Statistical Methods in Research and Production*. Oliver and Boyd, London (1961).
41. R. Byron Bird, W. E. Stewart and E. N. Lightfoot, *Transport Phenomena*. Wiley, New York (1960).